

Under Pressure: Learning to Detect Slip with Barometric Tactile Sensors

Abhinav Grover*, Christopher Grebe, Philippe Nadeau*, and Jonathan Kelly†

Abstract—The ability to perceive object slip through tactile feedback allows humans to accomplish complex manipulation tasks including maintaining a stable grasp. Despite the utility of tactile information for many robotics applications, tactile sensors have yet to be widely deployed in industrial settings—part of the challenge lies in identifying slip and other key events from the tactile data stream. In this paper, we present a learning-based method to detect slip using barometric tactile sensors. These sensors have many desirable properties including high reliability and durability, and are built from very inexpensive components. We are able to achieve slip detection accuracies of greater than 91% while displaying robustness to the speed and direction of the slip motion. Further, we test our detector on two robot manipulation tasks involving a variety of common objects and demonstrate successful generalization to real-world scenarios not seen during training. We show that barometric tactile sensing technology, combined with data-driven learning, is potentially suitable for many complex manipulation tasks such as slip compensation.

I. INTRODUCTION

Humans are able to perform complex dexterous manipulation tasks in part because of our rich tactile sensing capabilities. The sense of touch is essential to controlling the gripping force required to hold an object without slipping [1]. As part of humans’ sensory nervous system, a fast somatosensory feedback loop enables grasp adjustments to be performed within about 75 milliseconds, allowing for seamless and automatic grasp adaptation when handling a wide variety of objects in our daily lives [2]. Despite significant recent progress, artificial tactile sensors have yet to achieve the fidelity or accuracy of human tactile perception.

Tactile signals provide vital information about slip, that is, relative motion at the contact interface between the hand and an object, faster than any exteroceptive perception method. Slip can be disastrous (e.g., when transporting a fragile object) or advantageous (e.g., when moving an object without lifting it) depending on the context and the task [3]. In robotics, the well-studied “handover” task, which involves passing an object from a robot hand to a human hand, requires control of the gripping force with accuracy and speed to avoid significant slip [4]. The requisite feedback can only be provided through tactile sensing [5] and, consequently, the detection and control of slip events is fundamental to the completion of handovers and many other relevant tasks.

All authors are with the Space & Terrestrial Autonomous Robotics Systems (STARS) Laboratory at the University of Toronto Institute for Aerospace Studies, Toronto, Ontario, Canada. <firstname>. <lastname>@robotics.utias.utoronto.ca

*Abhinav Grover and Philippe Nadeau were supported in part by the Vector Institute Scholarship in Artificial Intelligence.

†Jonathan Kelly is a Vector Institute Faculty Affiliate. This research was supported in part by the Canada Research Chairs program.

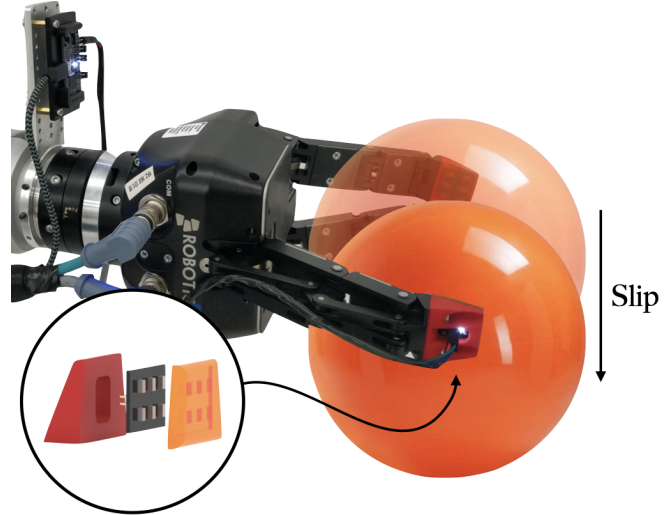


Fig. 1. We perform in-hand slip detection using barometric tactile sensors. Our approach involves training a temporal convolutional neural network (TCN) to recognize slip events directly from tactile data. The tactile sensors are mounted on the fingertips of a Robotiq 3-finger adaptive gripper. Inset: exploded view of each RightHand Labs TakTile sensor (plastic support frame, barometer circuit board, and rubber matrix, from left to right).

A wide range of new tactile sensors have become available over the last decade. These sensors measure various physical properties of the sensing interface including capacitance [6], impedance [7], or optical changes [8]–[11]. The BioTac fingertip, for example, is equipped with impedance-based tactile receptors, hydrophones, and thermistors to provide rich multimodal tactile information [7]. Each new tactile sensor has inherent characteristics such as fragility, bulk, resolution, nonlinearity, hysteresis, and production cost. Consideration of these characteristics and how they relate to varying task constraints leads to the best choice of tactile sensor for a specific job.

In this work we investigate the potential of low-cost tactile sensors assembled from off-the-shelf components, in combination with a state-of-the-art neural network, to perform slip detection. The sensors (the TakTile model from RightHand Labs) are built from an array of commercial MEMS barometers fixed to a PCB backplane, with a thin rubber matrix forming the contact surface. Although inexpensive, these sensors have a low profile, are mechanically robust, exhibit a consistent linear pressure response, and are easy to integrate with existing end-effectors.¹ The complex spatiotemporal signature of pressure changes during slip is difficult to model analytically—instead, we take a data-

¹The MEMS barometer used in this work (NXP MPL115A2) costs US\$2, approximately, per unit in quantities of 1,000 or more.

driven approach by training a temporal convolution neural network (TCN) to classify the time-series data produced by the tactile sensor as either static or slipping. To the best of the authors’ knowledge, this work is the first to use barometric tactile sensors for slip detection. We make the following contributions:

- an algorithm for slip detection using very low-cost barometric sensors that achieves an accuracy of over 90% on average;
- a comparison of our TCN approach with two other slip-detection methods that rely on vibration data;
- a preliminary analysis of the sensitivity and robustness of the TCN detector to factors related to surface properties and slipping motion;
- extensive experimental results for in-hand slip detection involving objects with various curvatures, hardnesses, and surface properties.

II. RELATED WORK

The study of tactile sensing for robotic systems has an extensive history, stretching back more than four decades (see, e.g., [12] and [13] for pioneering work). This research effort has been driven, in large part, by an evolving understanding of the essential role played by the sense of touch in human dexterous manipulation [14]. For a comprehensive review of existing sensors types, see [15]; a comprehensive review of slip detection, in turn, is provided by [16]. Due to limited space, we focus the remainder of our review below specifically on slip detection using tactile sensors.

Detecting slip is far from trivial. Some researchers have introduced signal-amplifying structures like rubber nibs or elastic ‘fingers,’ or combined several related sensing modalities, in an effort to make slip events easier to identify. In [17], data from a gripper-mounted tactile sensor are fused with measurements from a force-torque sensor to detect and control the slip of an object during manipulation. Similarly, the combination of a force-torque and a tactile sensor is used in [18] to detect incipient slip up to 100 ms before the slip occurs. The work of Goeger et al. [19] combines two tactile sensing modalities (piezoelectric and conductive polymer resistance changes) to generate ‘tactile features’ that are extracted from the fast Fourier transform (FFT) of the resulting signals. The features are grouped by a clustering algorithm to classify slip events [19]. In our work, we propose a method that uses static pressure readings only to infer whether an object is slipping, relaxing the need for an expensive force-torque sensor and also for high-frequency sampling.

Vision-based tactile sensors have seen significant development in recent years. These sensors infer tactile information from the visually-sensed deformation of the sensor contact surface. For two popular vision-based tactile sensors, the GelSight [20] and GelSlim [21], slip can be detected by monitoring changes to shear force at the contact surface. However, as noted in [22], the vision-based GelSight, GelSlim, and also the FingerVision sensor, can struggle to detect slip in certain situations due to a limited camera frame rate.

In [23], the TacTip sensor is modified to use a camera that operates at up to 120 frames per second so that rapid slip movements can be better identified. The authors of [23] train a support vector machine (SVM) classifier for slip detection, which performs with a high accuracy (>95%) for a wide range of slipping speeds. However, like most other vision-based sensor, this technology is bulky which prevents it from being used as anything other than fingertips. In contrast, barometric sensors are compact and can be easily distributed on the palm of a hand [24].

Methods for slip detection often rely on an analysis of the vibration pattern induced by object slip, where the frequency of the vibration (caused by material resonance) depends on the composition of the surfaces in contact. A detection approach developed by Holweg et al. [25] computes the power spectral density (PSD) of the piezoresistive tactile signal and feeds this data to a neural network to estimate the probability of slip. Dynamic sensing methods based on the analysis of the frequency spectrum of tactile signals can be sensitive to vibrations coming from the environment, such as those produced by nearby machinery; these vibrations have the potential to lead to the confounding of object-environment and object-gripper slip events. In [26], a dictionary of spectral tactile features is built to encode tactile readings and an SVM is trained to differentiate between object-environment and object-gripper slip. In Section V-A we compare the performance of a frequency-domain detection method to our proposed approach—our detector is able to operate reliably at a much lower data sampling frequency than in [27].

Due to the complex nature of tactile signals, data-driven approaches are increasingly being used for grasp stability assessment and slip detection [19], [21], [27]–[30]. The output of tactile sensors is often represented as 2D pressure images that are naturally suited for use as input to convolutional neural networks (CNNs). For instance, the work of Meier et al. [27] uses CNNs to detect slip events and differentiate between rotational and translational slip. Tactile signals also constitute time-series data that can be fed as inputs to recurrent neural networks (RNNs) [22], [31]–[33]. Experimental results in [34] suggests that temporal convolutional networks (TCN) can outperform conventional RNNs for a diverse set of sequence modeling tasks. This type of architecture has previously been used for audio synthesis [35] and for inertial measurement processing [36]. To the best of our knowledge, TCNs such as the one used in this work have not previously been applied to process the signals from tactile sensors.

III. SLIP DETECTION WITH BAROMETRIC SENSORS

Slip is a complex spatiotemporal event that is challenging to detect with any artificial tactile sensor. If barometric tactile sensors are to be used for this task within a learning framework, it is imperative that the detection model is trained with highly diverse examples. In this section we introduce our barometric tactile sensors and describe the slip data acquisition process that ensures data diversity, with the goal of improving generalization.

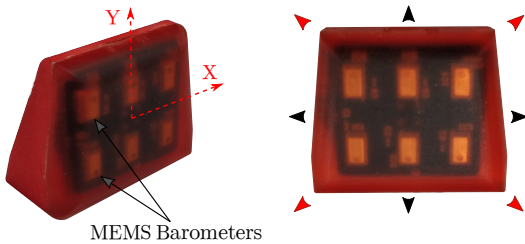


Fig. 2. Perspective (left) and front (right) view of the TakkTile fingertip. As part of the front view image, black arrows represent the primary sensor axes and red arrows represent the oblique axes.

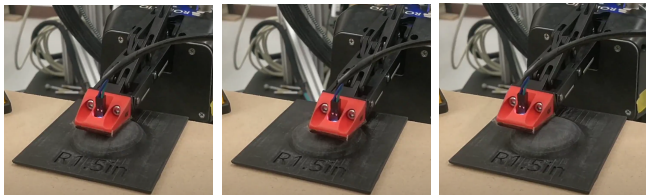


Fig. 3. TakkTile sensor mounted on the fingertip of our Robotiq gripper [37] and actuated automatically to slide over the 3D printed spherical surface during training data collection.

A. MEMS Barometric Tactile Sensors

We use an off-the-shelf TakkTile sensor kit, manufactured by RightHand Labs², for tactile sensing and slip detection. The kit includes three fingertip mounts designed to retrofit the *Robotiq* 3-finger gripper (Figure 1). The sensor design is based on the work of Tenzer et al. [37]. An array of commercial MEMS barometers (NXP MPL115A2) are assembled on a PCB and cast in a mold with urethane rubber, creating a flexible medium to transduce contact forces into barometric pressure signals. The layer of rubber is 10 mm thick; six MEMS barometers form a 2×3 sensing array spanning the contact region of each fingertips, as shown in Figure 2. Each TakkTile sensor provides pressure and temperature data at a sampling rate of 100 Hz, which is higher than that of most vision-based tactile sensors. The sensors are compact, robust, and very inexpensive relative to, for example, the competing BioTac sensors [7], while also exhibiting greater linearity ($<1\%$), no noticeable hysteresis, and a high signal-to-noise ratio (<0.01 N) [37].

B. Slip Data Acquisition

Our research is motivated, in part, by a desire to learn a general model of slip. To achieve this goal, it is essential that the slip detector is trained on data that spans many facets of object slip, such as slip speed and object curvature. We ensure diversity during data acquisition by collecting slip measurements using a UR10 robotic arm equipped with the Robotiq three-finger gripper mounted as an end-effector (shown in Figure 1). Additionally, a Robotiq FT300 force-torque (F/T) sensor is mounted at the wrist location. The TakkTile sensors replace the original fingertips of the gripper. A signal processing board provides synchronized pressure data over a USB interface. Using this actuation setup, we can move a TakkTile fingertip across fixed test surfaces



Fig. 4. Surfaces used for slip data acquisition; from left to right the images show a planer box lid, a spherical plastic surface (radius 1.5 in), and a cylindrical plastic surface (radius 2 in).

and generate a variety of customized slip scenarios; one collection trial is shown in Figure 3. The arm provides joint encoder measurements, which are used to determine the location of the fingertip through standard forward kinematics. At each time-step, the linear and angular velocity of the fingertip along the contact plane is calculated. Motions with translational and/or rotational velocities greater than 3 mm/s and 0.2 rad/s, respectively, are labelled as ‘slipping.’ These thresholds were determined empirically based on recordings of the TakkTile sensor under static conditions (i.e., resting on a surface without moving). Our setup allows for automation of the data collection process and ensures that the ground truth slip labels are accurate.

In the event of in-hand object slip, there are many factors related to the contact surfaces and slip motion itself that influence tactile sensor feedback. We identified five such factors, including material properties (e.g., roughness and rigidity), surface curvature, slip speed, slip direction, and normal contact force. Considering the huge variety of materials available, we focus our data collection efforts on the latter four factors and choose a common material with low coefficient of static friction: smooth rigid plastic. The generalization experiments in Section VI show that, although our network is trained using one material type, it is possible to reliably detect slip of objects made from a wide range of materials.

Since the UR10 arm does not support torque control, we instead use a PID controller that varies the position of the end-effector based on contact force feedback from the F/T sensor. Though the precision of the controller is not sufficient to maintain exact contact force during a slip maneuver, we are able to ensure surface contact throughout each motion. We 3D printed a section of a cylinder and a sphere in ABS plastic and sanded off the irregular edges to obtain smooth curved plastic surfaces, shown in Figure 4. For a planer surface, we use the lid of a smooth plastic box, which is also used for the robot experiments in Section VI. We programmed arm motions with a range of translational and rotational directions, including: an ‘asterisk’ maneuver, where the fingertip moves sequentially in eight different translation directions, and a ‘pendulum’ maneuver, where the gripper oscillates like a pendulum with the fingertip acting as the pivot point. For this work, we chose to collect slip data over surfaces with three different types of curvature (spherical, cylindrical, and planer), at three speed levels (0.05 m/s, 0.075 m/s, and 0.1 m/s), in eight different directions and while rotating the sensor clockwise and counterclockwise (see Figure 2); this range of motion covers the majority of

²Purchased from <https://www.labs.righthandrobotics.com/robotiq-kit>

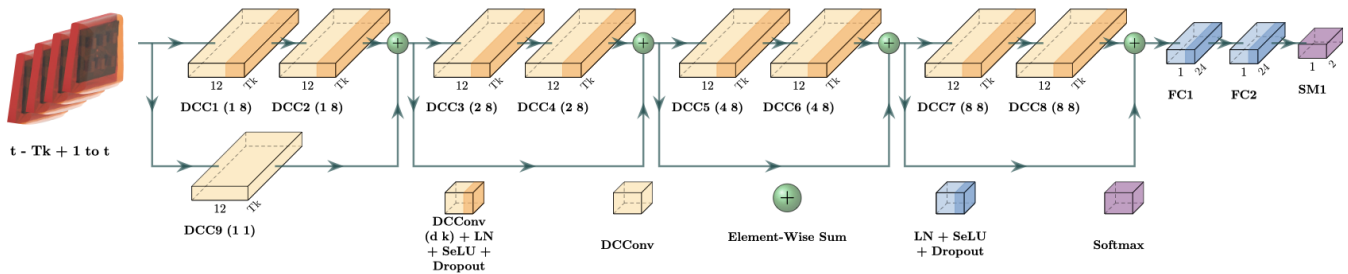


Fig. 5. The TCN [34] architecture used for slip detection, where temporal features are extracted using dilated convolution layers (DCC) [35]. For each DCC, d represents the dilation and k represents the kernel size. The next two layers are fully connected, followed by a softmax output for classification.

TABLE I

THE DISTRIBUTION OF TRAINING DATA BY SLIP TYPE. THE CYLINDRICAL SURFACE CAN BE FIXED IN TWO WAYS BASED ON THE ORIENTATION OF THE CYLINDER AXIS: ALONG THE X-AXIS AND ALONG THE Y-AXIS OF THE FINGERTIP SENSOR. THE MARGINALIZED DATA DISTRIBUTIONS ARE LISTED ON THE RIGHT AND BOTTOM OF THE TABLE.

Slip Type	Max. Speed	Planer	Spherical	Cylindrical (y -axis aligned)	Cylindrical (x -axis aligned)	
Translation (Primary Axes)	5 cm/s	5.3%	3.7%	3.5%	3.6%	16.1%
	7.5 cm/s	4.5%	4.7%	3.7%	3.7%	16.7%
	10 cm/s	4.8%	4.7%	3.3%	3.2%	15.9%
Translation (Oblique Axes)	5 cm/s	4.9%	3.3%	3.3%	3.3%	14.8%
	7.5 cm/s	3.5%	4.2%	3.5%	3.4%	14.5%
	10 cm/s	3.9%	4.2%	3.0%	3.1%	14.3%
Rotation	1 rad/s					
		30.7%	26.1%	21.7%	21.5%	

practical slip scenarios. The total data collected consist of over 45 minutes of TakkTile samples at a rate of 100 Hz, with 143,584 data points belonging to the static class and 122,918 data points belonging to the slip class. The data in the slip class is evenly distributed across slip speed, slip direction, and surface curvature, and includes both translational and rotational motions, as indicated in Table I. We applied a layer of cellophane tape over the fingertip during all experiments to prevent abrasive damage to the rubber surface.

IV. LEARNING TO DETECT SLIP

Prior research has successfully employed deep learning models to extract spatiotemporal features from tactile sensor data for slip detection [27], [32]. Given the superior performance of TCNs in comparison to recurrent architectures [34], we present a TCN-based architecture for slip detection.

A. Network Architecture

As shown in Figure 5, the input to the TCN is a stack of sensor values that constitute the last T_k seconds of tactile data. For our 100 Hz tactile sensors, we capture the last one second of data which makes the input an array of size 6×100 . We use a Keras implementation of the TCN [38] to extract temporal features from the array signals. The TCN layers are similar to the ones described in [34], except that we use layer normalization instead of weight normalization and SELU activations [39] instead of the ReLU activations. These architectural alterations are motivated by our experimental tests, which indicated better performance on the tactile dataset.

B. Training Details

The network is trained using the Adam optimizer [40] with a learning rate of 0.002 and a cross-entropy loss function. We use layer normalization, 20% dropout (for each layer including the fully connected layers), a mini-batch of size 256, and *He normal* [41] kernel initialization for network regularization. Moreover, at the beginning of each epoch we equalize the class distribution of the entire training dataset through random undersampling to prevent classification bias. The dataset was split into training (90%) and validation (10%) subsets, and the network was trained for 800 epochs. The validation data curves in Figure 6 show that a classification accuracy of more than 90% is achieved within fewer than 100 epochs.

C. Data Augmentation

The MEMS barometers, which are the primary transduction component of the barometric tactile sensors, form a 2×3 array on each fingertip module. We exploit the axial symmetry of the array to augment our data in order to reduce overfitting. Before each epoch, we randomly apply one of three transformations, an x -axis flip, a y -axis flip, or a 180° rotation, to every data point with a probability of 25% each. At the same time we add a small amount of random gaussian noise to the network inputs, with the intention of ensuring robustness to sensor noise.

V. SLIP DETECTION PERFORMANCE

We evaluated the performance of our method and compared it with prior work that utilizes contact pressure infor-

mation to detect slip. Additionally, we characterized the sensitivity of the detector to variations in the factors mentioned in Section III-B.

A. Performance Comparison

Although slip detection using barometric tactile sensors has not previously been attempted, there is prior work that employs other pressure transduction technologies. Holweg et al. [25] determine the power spectral density (PSD) of the vibrations induced in a piezoresistive rubber material by slip; the sum of the high-frequency PSD components is compared against a threshold to infer that slip has occurred. Meier et al. [27] train a CNN to classify slip events using data from an array of piezoresistive pressure sensors, where the data is first transformed into frequency domain ‘pressure images.’

For comparison purposes, we implemented our own versions of the methods in [25] and [27] and tested them on our dataset. We found the optimal PSD threshold by sweeping across various threshold values and evaluating the detector performance on the training dataset. To implement [27], we built a CNN with three times as many parameters as the TCN, using the last one second of sensor data as input (identical to the method proposed in this work) to calculate the frequency components, and generated input images of size 2×3 . We used the Adam optimizer, batch normalization, 20% dropout, class balancing, and data augmentation while training on the entire training set. Table II shows a performance comparison of the above two methods with our TCN-based approach. While both of the learning approaches demonstrate promising results, slip detection using the PSD threshold exhibits poor performance (as noted in [25] as well). The TCN outperformed the frequency CNN, with more than 5% improvement on each metric shown in Table II. Moreover, the TCN predicted the class label with significantly lower variance, according to the time-series plot shown in Figure 7. We believe the difference in the network performance can be attributed to the fact that Meier et al. [27] enforce a specific transformation for the temporal features in the sensor data, whereas the TCN learns to extract temporal features from the raw sensor outputs.

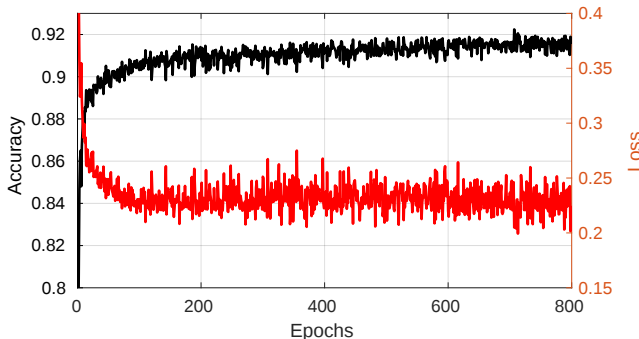


Fig. 6. Validation accuracy and loss curve during training of the TCN for 800 epochs over the entire training set.

TABLE II

PERFORMANCE COMPARISON BETWEEN TCN AND FREQUENCY-BASED METHODS ON TEST DATA. THE WEIGHTED AVERAGE OF THE CLASSES IS USED TO COMPUTE EACH METRIC.

Method	Accuracy	Precision	Recall	F1-Score
PSD Thresh. [25]	57.4%	57.9%	57.4%	57.5%
Freq. CNN [27]	86.0%	86.0%	86.0%	86.0%
TCN (ours)	91.3%	91.4%	91.4%	91.4%

B. Detection Sensitivity

The primary objective of this work is to create a highly accurate slip detector for barometric tactile sensors that can be used for real-world manipulation tasks. In this section, we evaluate the performance of the detector for possible combinations of slip type, slip speed, slip direction, and surface curvature, with the intention of characterizing the sensitivity of the detector. Table III summarizes the performance of the detector where we use the F1-score as a comparison.

It is clear from Table III that the performance of the detector is sensitive to material curvature, slip speed, and slip direction. The detector performs significantly better on planer surfaces in comparison to other surface curvatures. Additionally, the performance is better for cylindrical curvatures when the longitudinal cylinder axis is aligned with the x -axis of the fingertip, compared to the y -axis alignment case. The difference may be due to the fact that the TakkTile fingertip has only two rows of MEMS barometers in the y direction as opposed to three rows in the x direction. Performance of the detector appears to be correlated with the number of barometers strongly stimulated by the surface at a given time, which is why spherical and y -axis aligned cylindrical surfaces show worse performance. We note that performance improves as the slip speed is increased for almost all curvatures and slip directions, since higher speeds induce larger surface deformations and lead to more prominent temporal features within the one-second input time window. Performance is also affected by slip direction: slip along the oblique axes of the sensor is better detected than along the primary axes, although the difference is not significant for most slip speeds and curvatures. The detector produces good results ($>80\%$ F1-score) for rotational data as well, with the exception of spherical surfaces.

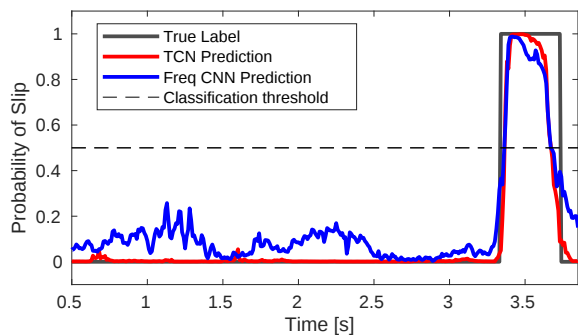


Fig. 7. Slip probability response of two detectors on test data. The fingertip was executing a translational slip maneuver on a spherical surface.

TABLE III

TCN PERFORMANCE, MEASURED BY F1-SCORE, WITH VARIATION IN SLIP TYPE, SLIP SPEED, SLIP DIRECTION, AND SURFACE CURVATURE.

	Max. Speed	Planer	Spherical	Cylindrical (y-axis aligned)	Cylindrical (x-axis aligned)	Curvature Independent
Translation (Primary Axes)	5 cm/s	92.5%	88.8%	78.7%	94.0%	89.7%
	7.5 cm/s	94.9%	88.0%	90.0%	90.3%	91.6%
	10 cm/s	95.7%	84.5%	87.8%	92.1%	93.1%
Translation (Oblique Axes)	5 cm/s	94.0%	88.9%	87.1%	93.2%	91.5%
	7.5 cm/s	96.6%	89.3%	93.7%	92.2%	93.1%
	10 cm/s	96.4%	88.6%	93.5%	93.4%	93.8%
Rotation	1 rad/s	84.6%	74.5%	84.0%	86.1%	81.5%
Motion Independent		94.0%	88.9%	88.0%	91.9%	

VI. ROBOT EXPERIMENTS

One of our main objectives is to train a detector which generalizes to common real-world slip detection tasks. We tested the generalization capabilities of our network model on the following two manipulation tasks: slip detection for an in-hand object under an externally-applied impulsive force, and slip detection while lifting an object with insufficient grasping force. The latter task was inspired by the work of James et al. [42], where slip is detected and compensated for during lifting. The test objects for the experiments (Figure 8) were selected with the intention of varying the properties of the contact surfaces, such as curvature, roughness and deformability. We note that these robot experiments demonstrate an ability to generalize from single-material training to real-world, multi-material slip detection involving different objects, a key contribution of our work.



Fig. 8. Test objects used for robot experiments. From left to right, the objects and their surface properties are: *plastic box* (planer, smooth, and rigid), *plastic ball* (spherical, smooth, and rigid), *football sleeve* (spherical, rough, and deformable), *foam sleeve* (cylindrical, smooth, and deformable), *metal can* (cylindrical, rough, and rigid), and *cardboard can* (cylindrical, smooth, and rigid). Note that the metal can is ribbed about its center.

A. Mallet Tap Test

The goal of this experiment was to evaluate the performance of the slip detector for in-hand objects held with a constant grasping force. For the test, we programmed the

robot arm and hand to grab an object with sufficient force to lift the object above the test table. The object was then manually tapped using a 16 oz rubber mallet with enough force to induce slip, but not to cause grasp failure. The setup for this test is shown in Figure 9; the LCD monitor in the background displayed slip events in real time. A slip state was registered only if the detection network produced a slip label for two consecutive time steps. A trial was deemed successful if slip was registered when the object was tapped, and the detector output returned to the nominal value (static) when the object stopped moving.

We conducted 20 trials per object, with an equal number of taps on the top and on the side of the object; the results are shown in Table IV. The slip detector achieved a success rate of 80% or more for each test object with an average accuracy of 87.5%. Slip detection for the foam sleeve, a very challenging object, had the worst performance, likely due to the smooth and deformable surface of the sleeve. Failure modes for this experiment included a nearly-equal number of false negatives and false positives, implying that the TCN does not exhibit any significant detection bias. The slip detector performed well under constant load conditions despite variations in material, curvature, deformability, and smoothness of the object surfaces. Since contact is maintained at all times, this test verifies that true object slip is being detected, rather than simply the detection of a uniform reduction in force across the tactile sensor array (i.e., a sudden ‘air gap’ upon grasping force reduction).

B. Object Lift Test

Lifting an object is a complicated task that requires precise hand-eye coordination and continuous adjustment to maintain a stable grasp. When lifting an object, humans intuitively change their grasping force based on the weight of the object. If a mismatch exists between the perceived and the actual weight, slip will occur due to insufficient grasping force. As an experiment, we replicated this scenario with our gripper and arm. For this task we used the same set of objects shown in Figure 8. Since the Robotiq gripper is not built for fine finger control, it was challenging to find gripper configurations that maintained contact with the object while generating insufficient grasping force. To solve this problem, we added weights to the lighter objects (i.e., the cardboard

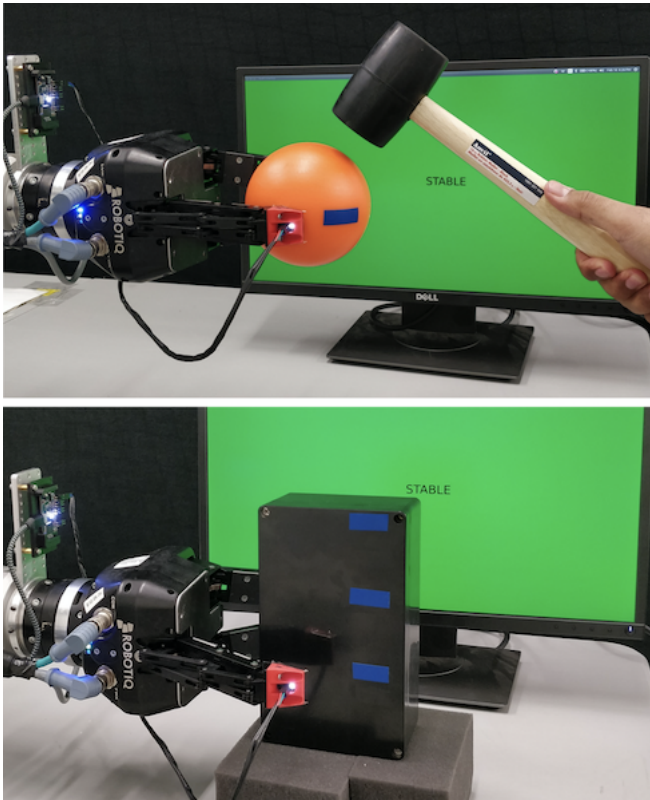


Fig. 9. Object mallet test for one trial with the plastic ball (top) and lift test for one trial with the plastic box (bottom). The blue tape on the objects marks the initial grasp location. The box has additional blue markings 6 and 12 cm above the initial grasp location for reference.

can, the football sleeve, and the foam sleeve) to increase the likelihood of slip. Figure 9 shows the setup used for this experiment. For the purpose of repeatability, we used a predetermined gripper configuration for each object and kept the initial grasping position consistent throughout the experiments. Once the gripper fingers reached a predetermined position, the slip detector was initialized—this was followed by a lifting motion. If slip was detected for two consecutive time steps, a slip event was registered and the gripper was programmed to tighten its grasp immediately in order to compensate. The task was particularly challenging for the slip detector because the normal contact force remained low throughout the lifting phase, despite the added weights.

An experimental trial was considered successful if slip was correctly detected and compensated for, that is, if the object was stably grasped and lifted up during the course of the hand motion. For the longer objects (namely the cardboard can, the plastic box, and the metal can), successful trials were split on the basis of the distance between the initial and the final grasp position—distance thresholds of 6 cm and 12 cm were used to define these two categories. We conducted 20 trials for each object; the experimental results are shown in Table IV. As a general trend, the success rate is greatest for longer objects, which we observed to be the result of reaction time: there is more time to ‘catch’ longer objects. Similarly, a high success rate was achieved with the football sleeve, which we attribute to its longer body and rough surface texture. Two

TABLE IV
SLIP DETECTION RESULTS FOR TWO REAL-WORLD MANIPULATION EXPERIMENTS.

Object	Mallet Tap	Object Lift
Plastic Ball	90%	35%
Plastic Box	85%	100% ³
Cardboard Can	90%	85% (45% ³ + 40% ⁴)
Football Sleeve	90%	85%
Foam Sleeve	80%	35%
Metal Can	90%	95% (75% ³ + 20% ⁴)
Avg. Success	87.5%	72.5%

³Final grasp within 6 cm of the initial grasp position.

⁴Final grasp between 6-12 cm of the initial grasp position.

prominent failure modes were observed for specific objects: failure due to slow reaction time (approx. 20 ms of which was required by the TCN), and failures in the form of false negatives. Given the smoothness and curvature of the plastic ball, it was impossible to stably grasp it anywhere except at its center. After a small amount of slip over a brief interval, the ball was off-centre relative to the gripper fingers, making a slower reaction time the dominant reason for failure. The smooth and compressible surface of the foam sleeve made it especially difficult to detect slip, leading to a large number of false negative results. We note, however, that deformable objects are generally very difficult to manipulate and that our detector was not trained with slip data from any.

VII. CONCLUSIONS AND FUTURE WORK

We presented a learning-based method for slip detection using inexpensive barometric tactile sensors. To demonstrate the accuracy and performance of our slip detection algorithm, we compared its performance with an existing classical method and a learning-based method. We ensured that our learned model was able to generalize by collecting diverse training data with variations in surface curvature, slip speed, slip direction, and slip type. Furthermore, we assessed the sensitivity and robustness of our method to the factors mentioned above. Finally, we evaluated the performance of the proposed slip detector on two real-world robotic manipulation tasks, using objects with different surface properties such as curvature, roughness, and deformability. Overall, our method achieved the best performance, with an accuracy of greater than 90% on a diverse dataset. The detector displayed high sensitivity to slip type and surface curvature, while being relatively robust to slip speed and direction. We also demonstrated that our learned model is able to transfer to real-world tasks (and to different materials) without retraining. Although better performance can sometime be achieved using other tactile sensors, barometric tactile sensors offer a unique combination of reliability, mechanical robustness, and price point, making them suitable for many industrial applications. We believe that the slip detection performance of barometric tactile sensors can be further improved by increasing the spatial density of the MEMS barometers on each fingertip (or at each grasp point).

As a continuation of this work, we would like to investigate the benefits of employing multiple TakTile fingertips

and a palm sensor for slip detection during manipulation. Similarly, the ability to estimate the type (translational or rotational) and direction of object slip would be valuable. Also, it would be interesting to explore control strategies for dexterous manipulation tasks that rely on controlled slip. Finally, we would like to examine the use of different barometric sensor configurations for tactile sensing, including as flexible ‘skin,’ similar to [24].

REFERENCES

- [1] G. Westling and R. Johansson, “Factors influencing the force control during precision grip,” *Experimental Brain Research*, vol. 53, no. 2, pp. 277–284, 1984.
- [2] R. S. Johansson and G. Westling, “Roles of glabrous skin receptors and sensorimotor memory in automatic control of precision grip when lifting rougher or more slippery objects,” *Experimental Brain Research*, vol. 56, no. 3, pp. 550–564, 1984.
- [3] C. Wang, S. Wang, B. Romero, F. Veiga, and E. Adelson, “SwingBot: Learning Physical Features from In-hand Tactile Exploration for Dynamic Swing-up Manipulation,” in *IEEE/RSJ Intl. Conf. Intelligent Robots and Systems (IROS)*, 2020, pp. 5633–5640.
- [4] V. Ortenzi, A. Cosgun, T. Pardi, W. Chan, E. Croft, and D. Kulić, “Object Handovers: a Review for Robotics,” *arXiv preprint arXiv:2007.12952*, 2020.
- [5] W. P. Chan, C. A. Parker, H. M. Van der Loos, and E. A. Croft, “Grip forces and load forces in handovers: implications for designing human-robot handover controllers,” in *Proc. ACM/IEEE Intl. Conf. Human-Robot Interaction*, 2012, pp. 9–16.
- [6] A. Maslyczyk, J.-P. Roberge, V. Duchaine, *et al.*, “A highly sensitive multimodal capacitive tactile sensor,” in *IEEE Intl. Conf. Robotics and Automation (ICRA)*, 2017, pp. 407–412.
- [7] R. S. Johansson, G. E. Loeb, N. Wettels, D. Popovic, and V. J. Santos, “Biomimetic tactile sensor for control of grip,” Feb. 1 2011, US Patent 7,878,075.
- [8] M. Lambeta, P.-W. Chou, S. Tian, B. Yang, B. Maloon, V. R. Most, D. Stroud, R. Santos, A. Byagowi, G. Kammerer, *et al.*, “DIGIT: A novel design for a low-cost compact high-resolution tactile sensor with application to in-hand manipulation,” *IEEE Robot. Autom. Lett.*, vol. 5, no. 3, pp. 3838–3845, 2020.
- [9] E. Donlon, S. Dong, M. Liu, J. Li, E. Adelson, and A. Rodriguez, “GelSlim: A high-resolution, compact, robust, and calibrated tactile-sensing finger,” in *IEEE/RSJ Intl. Conf. Intelligent Robots and Systems (IROS)*, 2018, pp. 1927–1934.
- [10] M. K. Johnson, F. Cole, A. Raj, and E. H. Adelson, “Microgeometry capture using an elastomeric sensor,” *ACM Trans. Graphics (TOG)*, vol. 30, no. 4, pp. 1–8, 2011.
- [11] C. Chorley, C. Melhuish, T. Pipe, and J. Rossiter, “Development of a tactile sensor based on biologically inspired edge encoding,” in *2009 Intl. Conf. on Advanced Robotics*, 2009, pp. 1–6.
- [12] R. S. Fearing and J. M. Hollerbach, “Basic Solid Mechanics for Tactile Sensing,” in *IEEE Intl. Conf. Robotics and Automation (ICRA)*, vol. 1, Atlanta, Georgia, USA, March 1984, pp. 266–275.
- [13] M. H. Raibert, “An All Digital VLSI Tactile Array Sensor,” in *IEEE Intl. Conf. Robotics and Automation (ICRA)*, vol. 1, Atlanta, Georgia, USA, March 1984, pp. 314–319.
- [14] R. S. Dahiya, G. Metta, M. Valle, and G. Sandini, “Tactile Sensing—From Humans to Humanoids,” *IEEE Trans. Robotics*, vol. 26, no. 1, pp. 1–20, February 2010.
- [15] M. R. Cutkosky and W. Provancher, “Force and tactile sensing,” in *Springer Handbook of Robotics*. Springer, 2016, pp. 717–736.
- [16] R. A. Romeo and L. Zollo, “Methods and sensors for slip detection in robotics: a survey,” *IEEE Access*, April 2020.
- [17] C. Melchiorri, “Slip detection and control using tactile and force sensors,” *IEEE/ASME Trans. Mechatronics*, vol. 5, no. 3, pp. 235–243, 2000.
- [18] N. Jamali and C. Sammut, “Slip prediction using hidden Markov models: Multidimensional sensor data to symbolic temporal pattern learning,” in *IEEE Intl. Conf. Robotics and Automation (ICRA)*, 2012, pp. 215–222.
- [19] D. Goeger, N. Ecker, and H. Woern, “Tactile sensor and algorithm to detect slip in robot grasping processes,” in *IEEE Intl. Conf. Robotics and Biomimetics*, 2009, pp. 1480–1485.
- [20] W. Yuan, R. Li, M. A. Srinivasan, and E. H. Adelson, “Measurement of shear and slip with a GelSight tactile sensor,” in *IEEE Intl. Conf. Robotics and Automation (ICRA)*, 2015, pp. 304–311.
- [21] S. Dong, D. Ma, E. Donlon, and A. Rodriguez, “Maintaining Grasps within Slipping Bounds by Monitoring Incipient Slip,” in *IEEE Intl. Conf. Robotics and Automation (ICRA)*, 2019, pp. 3818–3824.
- [22] Y. Zhang, W. Yuan, Z. Kan, and M. Y. Wang, “Towards Learning to Detect and Predict Contact Events on Vision-based Tactile Sensors,” in *Conf. on Robot Learning (CORL)*, vol. 100. Proceedings of Machine Learning Research, 2020, pp. 1395–1404.
- [23] J. W. James and N. F. Lepora, “Slip Detection for Grasp Stabilization With a Multifingered Tactile Robot Hand,” *IEEE Trans. Robotics*, 2020.
- [24] R. Koiva, T. Schwank, G. Walck, M. Meier, R. Haschke, and H. Ritter, “Barometer-based Tactile Skin for Anthropomorphic Robot Hand,” in *IEEE/RSJ Intl. Conf. Intelligent Robots and Systems (IROS)*, 2020, pp. 9821–9826.
- [25] E. Holweg, H. Hoeve, W. Jongkind, L. Marconi, C. Melchiorri, and C. Bonivento, “Slip detection by tactile sensors: algorithms and experimental results,” in *IEEE Intl. Conf. Robotics and Automation (ICRA)*, vol. 4, 1996, pp. 3234–3239.
- [26] J.-P. Roberge, S. Rispal, T. Wong, and V. Duchaine, “Unsupervised feature learning for classifying dynamic tactile events using sparse coding,” in *IEEE Intl. Conf. Robotics and Automation (ICRA)*, 2016, pp. 2675–2681.
- [27] M. Meier, F. Patzelt, R. Haschke, and H. J. Ritter, “Tactile Convolutional Networks for Online Slip and Rotation Detection,” in *Intl. Conf. Artificial Neural Networks (ICANN)*, 2016, pp. 12–19.
- [28] E. Hyttinen, D. Kragic, and R. Detry, “Learning the tactile signatures of prototypical object parts for robust part-based grasping of novel objects,” in *IEEE Intl. Conf. Robotics and Automation (ICRA)*, 2015, pp. 4927–4932.
- [29] H. Dang and P. K. Allen, “Stable grasping under pose uncertainty using tactile feedback,” *Autonomous Robots*, vol. 36, no. 4, pp. 309–330, 2014.
- [30] J. Kwiatkowski, D. Cockburn, and V. Duchaine, “Grasp stability assessment through the fusion of proprioception and tactile signals using convolutional neural networks,” in *IEEE/RSJ Intl. Conf. Intelligent Robots and Systems (IROS)*, 2017, pp. 286–292.
- [31] F. Veiga, J. Peters, and T. Hermans, “Grip Stabilization of Novel Objects Using Slip Prediction,” *IEEE Trans. on Haptics*, vol. 11, no. 4, pp. 531–542, Oct 2018.
- [32] B. S. Zapata-Impata, P. Gil, and F. Torres, “Tactile-driven grasp stability and slip prediction,” *Robotics*, vol. 8, no. 4, p. 85, dec 2019.
- [33] P. Nadeau, M. Abbott, D. Melville, and H. S. Stuart, “Tactile sensing based on fingertip suction flow for submerged dexterous manipulation,” in *IEEE Intl. Conf. Robotics and Automation (ICRA)*, 2020, pp. 3701–3707.
- [34] S. Bai, J. Z. Kolter, and V. Koltun, “An empirical evaluation of generic convolutional and recurrent networks for sequence modeling,” *arXiv preprint arXiv:1803.01271*, 2018.
- [35] A. van den Oord, S. Dieleman, H. Zen, K. Simonyan, O. Vinyals, A. Graves, N. Kalchbrenner, A. Senior, and K. Kavukcuoglu, “WaveNet: A Generative Model for Raw Audio,” in *ISCA Speech Synthesis Workshop*, 2016, pp. 125–125.
- [36] E. Kaufmann, A. Loquercio, R. Ranftl, M. Mueller, V. Koltun, and D. Scaramuzza, “Deep Drone Acrobatics,” *Robotics: Science and Systems (RSS)*, 2020.
- [37] Y. Tenzer, L. P. Jentoft, and R. D. Howe, “The Feel of MEMS Barometers: Inexpensive and Easily Customized Tactile Array Sensors,” *IEEE Robot. Autom. Mag.*, vol. 21, no. 3, pp. 89–95, 2014.
- [38] P. Remy, “Temporal Convolutional Networks for Keras,” Github, 2020. [Online]. Available: <https://github.com/philipperemy/keras-tcn>.
- [39] A. M. Günter Klambauer, Thomas Unterthiner and S. Hochreiter, “Self-Normalizing Neural Networks,” in *Advances in Neural Information Processing Systems (NeurIPS)*, 2017, pp. 972–981.
- [40] D. P. Kingma and J. Ba, “Adam: A method for stochastic optimization,” *arXiv preprint arXiv:1412.6980*, 2014.
- [41] K. He, X. Zhang, S. Ren, and J. Sun, “Delving deep into rectifiers: Surpassing human-level performance on imagenet classification,” in *Intl. Conf. Computer Vision (ICCV)*, 2015, pp. 1026–1034.
- [42] J. W. James, N. Pestell, and N. F. Lepora, “Slip Detection With a Biomimetic Tactile Sensor,” *IEEE Robot. Autom. Lett.*, vol. 3, no. 4, pp. 3340–3346, 2018.